High-energy photon-nucleon and photon-nucleus cross sections

Katsuhiko Honjo* and Loyal Durand†
Department of Physics, University of Wisconsin–Madison, Madison, Wisconsin 53706

Raj Gandhi‡
Department of Physics, Texas A&M University, College Station, Texas 77843

Hong Pi§
Department of Theoretical Physics, University of Lund, Lund, Sweden S-22362

Ina Sarcevic**
Department of Physics, University of Arizona, Tucson, Arizona 85721
(Received 22 December 1992)

We reexamine the theory of hadronic photon-nucleon interactions at the quark-gluon level. The possibility of multiple parton collisions in a single photon-nucleon collision requires an eikonal treatment of the high-energy scattering process. We give a general formulation of the theory in which the γp cross section is expressed as a sum over properly eikonalized cross sections for the interaction of the virtual hadronic components of the photon with the proton, with each cross section weighted by the probability with which that component appears in the photon, and then develop a detailed model which includes contributions from light vector mesons and from excited virtual states described in a quark-gluon basis. The parton distribution functions which appear can be related approximately to those in the pion, while a weighted sum gives the distribution functions for the photon. We use the model to make improved QCD-based predictions for the total inelastic photon-nucleon and photon-nucleus cross sections at energies relevant for DESY HERA experiments and cosmic-ray observations. We emphasize the importance in this procedure of including a soft-scattering background such that the calculated cross sections join smoothly with low-energy data. Our results show clearly that high-energy measurements of the total inelastic γp cross section can impose strong constraints on the gluon and quark distributions in the photon, and indirectly on those in the pion.

PACS number(s): 13.60.Hb, 12.40.Pp, 13.87.Ce

I. INTRODUCTION

The high-energy "hadronic" interactions of the photon are currently a subject of considerable experimental and theoretical interest. The virtual quark-gluon structure of the photon can lead to a significant inclusive jet cross section in high-energy γp collisions. This cross section and the quark and gluon distributions in the photon will be measurable in future experiments at the electron-proton collider HERA at DESY [1–3]. It is useful in that context to have predictions [3] for the total inelastic γp cross section through the HERA energy range. The hadronic interactions of the photon in very-high-energy photon-nucleon and photon-nucleus collisions have also been studied recently [4–7] in the context of reports of anomalously high muon content in PeV cosmic-ray air showers [8]. These showers were apparently initiated by photons from point sources of cosmic rays. However, their reported muon content was up to an order of magnitude higher than expected in electromagnetic showers, and approached that typical of proton-initiated hadronic showers. This suggested that the hadronic structure of the photon might play a role [4], an idea which has been investigated in detail [5–7].

Although it now appears that "hadronic" photon-nucleus interactions with realistic photon structure functions cannot account for the apparent muon anomalies [6]—and the cosmic-ray observations have so far not been confirmed—theoretical questions with respect to the proper calculation of photon-nucleon and photon-nucleus cross sections remain. In particular, the large numbers of partons (quarks and gluons) present in the photon and nucleons at very high energies make multiple parton-parton collisions likely in a single γ-nucleon interaction, and can lead to violations of partial-wave unitarity in simplified calculations. An eikonal treatment of the scattering amplitude is necessary to remove this problem. It was pointed out recently by Collins and Ladinsky [9] that the method of eikonalization used in previous work [6] was incorrect. Those calculations treated the hadronic photon similarly to any other hadron, and used the formalism developed for nucleon-nucleon scattering [10] to describe the photon-nucleon interaction. However, the photon is not like an ordinary hadron which always ex-

*Electronic address: honjo@wishep.bitnet
†Electronic address: ldurand@wishep.bitnet
‡Electronic address: raj@tamphys.bitnet
§Electronic address: pihong@thep.lu.SE
**Electronic address: ina@arizvms.bitnet

ists in a hadronic state consisting of quarks and gluons. The photon is usually in a bare or nonhadronic state with respect to the strong interactions and only turns into a virtual $q\bar{q}$ pair occasionally, with a total probability $\mathcal{P}_{\rm had} \ll 1$. The eikonalization should apply only to the scattering of the resulting hadronic system. The probability that the photon is in any particular hadronic state should therefore appear as an overall factor in the contribution of that state to $\sigma_{\gamma p}$, and must be extracted from the corresponding eikonal function.

Collins and Ladinsky [9] estimated $\mathcal{P}_{\rm had}$ using the vector dominance model with only the lightest vector states included, with the result

$$\mathcal{P}_{\rm had}^{\rm CL} = \frac{4\pi\alpha_{\rm em}}{f_\rho^2} \approx \frac{1}{300}. \tag{1}$$

It was assumed that this factor could simply be divided out of the QCD contributions to the eikonal function as defined in earlier work, and included as an overall factor in $\sigma^{\gamma p}$ as noted above. Following this line of reasoning, Collins and Ladinsky [9], Fletcher, Gaisser, and Halzen [11], and Forshaw and Storrow [12] recomputed the γp total inelastic cross section up to cosmic-ray energies and found it to be considerably smaller than previously suggested [4–6].

We have also reexamined this question and have improved earlier predictions [3] for the photon-nucleon and photon-nucleus cross sections at energies relevant to projects at HERA, and also the cosmic-ray observations [6]. In the process, we have considerably improved the theoretical treatment of the problem [13]. The γp cross section is now expressed as a weighted sum of eikonalized cross sections for the interactions of the hadronic components of the photon with the proton. The weights are the probabilities with which those virtual components appear in the physical photon. We have developed a detailed model which includes contributions from light vector mesons and from excited virtual states with the latter described in a quark-gluon basis. The "soft" contributions to the eikonal functions are parametrized in the form expected from Regge theory to assure that the calculated high-energy cross sections connect smoothly with the cross sections measured at lower energies. The parton distribution functions which appear in the "hard-scattering" contributions to the eikonal functions can be related approximately to those in the pion. This approach allows us to use the (not-well-determined) pion distributions to predict the high-energy behavior of the γp cross section, and also gives an approximate prediction for the parton distributions in the photon in terms of these in the pion. We also develop an alternative approach based directly on the photon distribution functions, but find that the simple approximations used in [9, 11, 12] must be modified.

We find, in accord with the results of other authors [9, 11, 12], that the inelastic γp cross section is strongly suppressed at high energies relative to results reported earlier [4–7]. The new results on γ-air interactions make it quite clear that the hadronic interactions of the photon cannot explain the reported muon anomalies in cosmic-ray showers, if the anomalies in fact exist. However, the QCD contributions to the hadronic interactions of the photon still lead to a rapid rise in $\sigma^{\gamma p}$ at HERA energies as predicted in earlier calculations [3] and observed in recent experiments [14]. The magnitude of the rise provides a quantitative test of the whole picture. In particular, our results show clearly that measurements of the total inelastic γp cross section at HERA can impose strong constraints on the parton distributions in the photon, and indirectly on those in the pion.

In the following sections, we sketch the theoretical background of our calculations (Sec. II), discuss the detailed model (Sec. III), and present our calculations and conclusions (Sec. IV).

II. THEORETICAL BACKGROUND

Physical photon state and the γp cross section

As noted above, the hadronic interactions of the photon are different from those of ordinary hadrons in that the photon exists in a hadronic state only with a small total probability $\mathcal{P}_{\rm had}$. In the presence of the strong interactions, but neglecting purely electromagnetic effects, the incoming physical photon in a γp scattering process can be described perturbatively as a superposition of a "bare" photon and a set of virtual hadronic states,

$$|\gamma\rangle_{\rm phys} = (1-\mathcal{P}_{\rm had})^{1/2}|\gamma\rangle_{\rm bare} + \sum_m{}'|m\rangle\frac{\langle m|H_I|\gamma\rangle}{E_\gamma - E_m}, \tag{2}$$

where $H_I = H_I(\mathbf{x}, 0)$ is the $\gamma q\bar{q}$ interaction:

$$H_I = j\cdot A = e\sum_q e_q\bar{\psi}_q \not{A}\psi_q(\mathbf{x},0). \tag{3}$$

The sum is restricted to hadronic states which can be treated as real incoming states in a subsequent scattering, that is, to states which last a time long relative to the time necessary for the photon to traverse the target proton or the relevant structures in it, and hence are almost on shell. The "bare" state $|\gamma\rangle_{\rm bare}$ includes the short-lived hadronic fluctuations which cannot be distinguished in the γp interaction. The probability with which an observable hadronic state $|m\rangle$ appears in $|\gamma\rangle_{\rm phys}$ is simply

$$\mathcal{P}_m = \frac{|\langle m|H_I|\gamma\rangle|^2}{(E_\gamma - E_m)^2} \tag{4}$$

and

$$\mathcal{P}_{\rm had} = \sum_m{}'\mathcal{P}_m. \tag{5}$$

Given this structure, the inelastic γp cross section will be given approximately as a sum of cross sections,

$$\sigma_{\rm inel}^{\gamma p} = (1-\mathcal{P}_{\rm had})\sigma_{\rm dir} + \sum_m{}'\mathcal{P}_m\sigma_m. \tag{6}$$

The first term represents the inelastic interaction of the bare photon directly with the proton (or the quarks and gluons in it); the sum includes the interactions of the

quasireal intermediate hadronic states with the proton. We neglect possible interference terms involving final states which can be reached from distinct initial configurations. We expect these to give very small average contributions.

There are no rescattering corrections to the direct-interaction cross section $\sigma_{\rm dir}$ to lowest order in the electromagnetic coupling $\alpha_{\rm em}$, and $\sigma_{\rm dir}$ can simply be identified at high energies and momentum transfers with the inclusive direct-interaction cross section of QCD:

$$\sigma_{\rm dir}^{\rm QCD} = \sum_i \int_0^1 dx \int_{p_{\perp,\rm min}^2} dp_\perp^2 \, f_i^p(x,p_\perp^2) \, \frac{d\hat{\sigma}_{\gamma i}}{dp_\perp^2}(\hat{s},p_\perp^2). \tag{7}$$

Here the f's are the number distributions of the quarks, antiquarks, and gluons in the proton, $d\hat{\sigma}_{\gamma i}/dp_\perp^2$ is the relevant differential γ-parton scattering cross section, and $\hat{s}$ is the invariant mass of the γ-parton system. The lower bound $p_{\perp,\rm min}$ on the transverse momentum $p_\perp$ in the scattering parametrizes the point at which semihard and soft processes merge.

The theoretical problem at this point involves the calculation of the probabilities $\mathcal{P}_m$ and the hadronic cross sections σ_m in Eq. (6). The low-mass hadronic states in the sum are just the vector-meson states ρ, ω, ϕ. These are normal hadronic states produced with probabilities [15]

$$\mathcal{P}_V = \frac{4\pi\alpha_{\rm em}}{f_V^2}, \tag{8}$$

where f_V is the γV coupling in the effective Hamiltonian of the vector dominance model:

$$H_{\gamma V} = \frac{e}{f_V} m_V^2 \mathbf{A}\cdot\mathbf{V} \, . \tag{9}$$

The scattering of the vector mesons can be described using the eikonal methods developed for high-energy nucleon-nucleon [10] or meson-nucleon [16] scattering as discussed below. We will treat the ρ and ω as equivalent, and will use the quark-model ratios for the couplings f_V. The contribution of the low-mass vector mesons to the sum in Eq. (6) is then

$$\sum_V \mathcal{P}_V \sigma_V = \lambda \mathcal{P}_\rho \sigma_\rho = \lambda \frac{4\pi\alpha_{\rm em}}{f_\rho^2}\sigma_\rho, \tag{10}$$

where σ_ρ is the inelastic ρp scattering cross section, $\lambda = 4/3$ for equal ρp, ωp, and ϕp cross sections, and $\lambda = 10/9$ for complete suppression of the ϕ contribution [17].

There is no strong resonance structure observed in the vector $u\bar{u}$, $d\bar{d}$, and $s\bar{s}$ channels at higher masses, but many possible nonresonant final states exist in inelastic γp scattering. In this situation the relevant hadronic states in Eq. (6) are best described inclusively in a quark-gluon basis. We begin by considering the initial transition $\gamma \to q\bar{q}$. We write the four-momenta k, p, and p' of the photon, quark, and antiquark in terms of longitudinal and transverse components as

$$\begin{aligned} k &= (k, \mathbf{0}_\perp, k), \\ p &= \left(\sqrt{(xk)^2 + p_\perp^2}, \mathbf{p}_\perp, xk\right), \\ p' &= \left(\sqrt{(1-x)^2k^2 + p_\perp^2}, -\mathbf{p}_\perp, (1-x)k\right), \end{aligned} \tag{11}$$

where $\mathbf{k}\cdot\mathbf{p}_\perp = 0$ and $x = \mathbf{p}\cdot\hat{\mathbf{k}}/|\mathbf{k}|$ is the fraction of the (purely longitudinal) three-momentum of the photon which is carried by the quark. The differential transition probability $d\mathcal{P}_{q\bar{q}}$ for $\gamma \to q\bar{q}$ is then given for xk, $(1-x)k \gg p_\perp$ and one flavor of quark by

$$d\mathcal{P}_{q\bar{q}} = \frac{3\alpha_{\rm em}e_q^2}{2\pi}\frac{1}{p_\perp^2}\left[x^2 + (1-x)^2\right] dx dp_\perp^2. \tag{12}$$

With the same kinematic approximations, $p_\perp$ and the invariant mass M of the $q\bar{q}$ pair are related by

$$M^2 = (E+E')^2 - \mathbf{k}^2 = p_\perp^2/x(1-x) \ll \mathbf{k}^2 \, . \tag{13}$$

The lifetime of a $q\bar{q}$ system with mass M is given approximately by

$$\tau \approx 1/(E + E' - E_\gamma) \approx 2k/M^2 \, . \tag{14}$$

The average longitudinal separation of the quarks during the lifetime of the system,

$$\begin{aligned} r_\parallel &\approx \frac{1}{2}\tau v_{\parallel,\rm relative} \\ &\approx \frac{1}{2}\tau\left(\frac{xk}{E} - \frac{(1-x)k}{E'}\right) \approx \frac{1}{2k}\frac{2x-1}{x(1-x)} \, , \end{aligned} \tag{15}$$

is much smaller than the average transverse separation:

$$r_\perp = \frac{1}{2}\tau\left(\frac{p_\perp}{E} - \frac{(-p_\perp)}{E'}\right) \approx \frac{1}{p_\perp} \tag{16}$$

for $p_\perp \ll k$. If $r_\perp$ is greater than, or on the order of, the average transverse radius $R_\perp$ of a vector meson, QCD confinement effects will clearly set in, and the $q\bar{q}$ system will appear in a hadronic collision as a "soft" system with a typical hadronic size and interactions, e.g., as a light vector meson. On the other hand, for $r_\perp < R_\perp$, the system of quark, antiquark, and the connecting color flux tube will be smaller than a vector meson during its transit through the target. It may still interact softly with the target, but with an intrinsic cross section which is reduced by a geometrical factor of order $(r_\perp/R_\perp)^2 \approx (1/p_\perp R_\perp)^2$ for large initial values of $p_\perp$. The high-momentum-transfer branching processes of perturbative QCD lead to higher transverse velocities but shorter intermediate lifetimes, and to only a small average increase in the size of the system.

We can estimate $R_\perp$ using the expected similarity of the ρ and π meson wave functions [18] and experimental results on the pion electromagnetic form factor. The measured parameter $\mu^2 = 0.47$ (GeV/c)^2 [19] in the series representation of the form factor

$$G_\pi(Q^2) = 1 - Q^2/\mu^2 + \cdots \tag{17}$$

corresponds to a root-mean-square transverse radius

$$\langle r_\perp^2 \rangle_\pi^{1/2} = 2/\mu \approx (350 \text{ MeV})^{-1}. \quad (18)$$

We will identify $R_\perp$ with this radius. Under this assumption, the vector-meson-like behavior will hold for initial values of $p_\perp$ less than about 350 MeV. This value corresponds to an average mass of the system $\langle M \rangle = \frac{9\pi}{8} p_\perp \approx 1.2$ GeV, where the average is over the x distribution in Eq. (12). This mass is comfortably between the masses of the $\rho(770)$ and $\omega(783)$, which we are taking into account explicitly, and the $\rho(1450)$, which we are not. However, it is sufficiently close to the mass of the $\phi(1020)$ that ϕ production, which involves the relatively massive strange quarks, could be suppressed, a possibility which we will consider later. In the following discussion we will adopt the value $Q_0 = \mu/2 \approx 350$ MeV/c for the critical value of $p_\perp$ above which the hadronic states are no longer describable as vector mesons. The precise value of this parameter will not be essential.

Our expression for the inelastic γp cross section is given at this point by

$$\sigma_{\text{inel}}^{\gamma p} = (1 - \mathcal{P}_{\text{had}})\sigma_{\text{dir}} + \lambda \mathcal{P}_\rho \sigma_\rho + \int_{Q_0^2} d\mathcal{P}_{q\bar{q}}(x_0, p_{\perp 0}^2)\sigma_{q\bar{q}}, \quad (19)$$

where $\mathcal{P}_{\text{had}}$ may be dropped in the first term to leading order in α_{em}. The integral in the last term is over the initial values of x and $p_\perp$ for the $q\bar{q}$ pair. The condition that the intermediate hadronic state have a lifetime long compared to the time necessary to traverse the target imposes an upper limit on the integrations given by

$$\tau \approx 2k/M^2 = 2kx(1-x)/p_\perp^2 \gg R\,, \quad (20)$$

where R is the radius of the target. Thus,

$$p_\perp^2 \ll 2kx(1-x)/R \leq k/2R. \quad (21)$$

This limit has little effect at high energies because of the $1/p_\perp^2$ decrease of $\sigma_{q\bar{q}}$ at large momentum transfers, and we will ignore it. For simplicity, we will also ignore the possible dependence of $\sigma_{q\bar{q}}$ on x_0. Then, using the expression in Eq. (12) and integrating over x_0, we find that, to leading order in α_{em} [20],

$$\sigma_{\text{inel}}^{\gamma p} = \sigma_{\text{dir}}^{\text{QCD}} + \lambda \mathcal{P}_\rho \sigma_\rho + \sum_q e_q^2 \frac{\alpha_{\text{em}}}{\pi} \int_{Q_0^2} \frac{dp_{\perp 0}^2}{p_{\perp 0}^2} \sigma_{q\bar{q}}(s, p_{\perp 0}^2). \quad (22)$$

In the next section, we discuss the calculation of the hadronic cross sections σ_ρ and $\sigma_{q\bar{q}}$.

III. ESTIMATES FOR THE HADRONIC CROSS SECTIONS

A. Vector-meson cross sections

The ρp cross section and the lower-mass $q\bar{q}p$ cross sections in Eq. (22) are of hadronic magnitude, and are best treated at high energies using an eikonal formalism. We will follow the methods discussed in detail in [10] and [16], and write a typical hadronic cross section in Eq. (22) as

$$\sigma_m(s) = 2 \int d^2b \left(1 - e^{-\text{Re}\chi_m(b,s)}\right). \quad (23)$$

Semiclassically, $e^{-2\text{Re}\chi}$ is the probability that the two incoming systems (the proton and the virtual hadronic component $|m\rangle$ of the photon) survive a collision at impact parameter b. We will write the eikonal function χ as the sum of two terms corresponding to contributions from "soft" and "hard" or low- and high-momentum-transfer processes,

$$\text{Re}\chi = \text{Re}\chi_{\text{soft}} + \text{Re}\chi_{\text{QCD}}. \quad (24)$$

In the case of the ρ meson, we are dealing with a normal hadron, and familiar arguments [10] can be used to relate the hard component of χ to $\sigma_{\text{QCD}}^{\rho p}$, the inclusive parton-level cross section for ρp scattering:

$$2\text{Re}\chi_{\text{QCD}}^{\rho p}(b,s) = A_{\rho p}(b)\sigma_{\text{QCD}}^{\rho p}. \quad (25)$$

Since the QCD cross section is dominated by small-angle scattering, we will use an expression appropriate to that region:

$$\sigma_{\text{QCD}}^{\rho p} = \sum_{ij} \int_0^1 dx_1 \int_0^1 dx_2 \int_{p_{\perp,\min}^2} dp_\perp^2 f_i^p(x_1, p_\perp^2) f_j^\rho(x_2, p_\perp^2) \frac{d\hat{\sigma}_{ij}}{dp_\perp^2}\,, \quad p_\perp^2 < \hat{s}/4. \quad (26)$$

Here f^p and f^ρ give the parton distributions in the proton and ρ meson, and $d\hat{\sigma}_{ij}/dp_\perp^2$ is the cross section for the scattering of partons i and j. The proton structure functions are well known [21]. We will return later to a discussion of the structure functions for the ρ meson. $A_{\rho p}(b)$ is the parton density overlap function, expressed as the convolution of the normalized transverse parton densities in the ρ meson and the proton,

$$A_{\rho p}(b) = \int d^2b' \rho_\rho(b)\rho_p(|\mathbf{b} - \mathbf{b}'|)\,, \qquad \int d^2b A_{\rho p}(b) = 1. \quad (27)$$

The density $\rho_p(b)$ can be taken as the Fourier transform of the proton electromagnetic charge form factor:

$$G_E\left(k_\perp^2\right) \approx \left(1 + \frac{k_\perp^2}{\nu^2}\right)^{-2}, \qquad \nu^2 = 0.71 \text{ GeV}^2, \quad (28)$$

a choice which works well in the case of pp [22] and $\bar{p}p$ scattering [10]. Then

$$\rho_p(b) = \frac{1}{(2\pi)^2} \int d^2k_\perp G_p\left(k_\perp^2\right) e^{i\mathbf{k}_\perp \cdot \mathbf{b}} = \frac{1}{4\pi}\nu^2(\nu b)K_1(\nu b), \quad (29)$$

where $K_n(x)$ is the exponentially decreasing hyperbolic Bessel function [23].

For the ρ meson, we use the density given by the Fourier transform of the (less-well-known) pion form factor, since it is expected to be essentially the same as that of the ρ meson in the quark model [16, 18]. The density $\rho_\rho(b)$ is then given by an expression similar to that in the first line in Eq. (29), but with [19]

$$G_\rho(k_\perp^2) \approx G_\pi(k_\perp^2) \approx \left(1+\frac{k_\perp^2}{\mu^2}\right)^{-1}, \qquad \mu^2 = 0.47\ \mathrm{GeV}^2. \tag{30}$$

With this input,

$$\rho_\rho(b) \approx \frac{\mu^2}{2\pi} K_0(\mu b) \tag{31}$$

and [16]

$$A_{\rho p}(b) = \frac{1}{4\pi}\frac{\nu^2\mu^2}{\mu^2-\nu^2}\left\{\nu b K_1(\nu b) - \frac{2\nu^2}{\mu^2-\nu^2}[K_0(\nu b)-K_0(\mu b)]\right\}. \tag{32}$$

The incident hadronic systems in a ρp collision can interact inelastically through soft as well as hard processes, hence the presence of first term in Eq. (24). This soft scattering is dominant at the energies explored so far. We will parametrize $\mathrm{Re}\,\chi_{\mathrm{soft}}$ using the same overlap function as above multiplied by an energy-dependent factor with a form suggested by Regge theory:

$$2\mathrm{Re}\,\chi_{\mathrm{soft}} = A_{\rho p}(b)\sigma_{\mathrm{soft}}(s), \tag{33}$$

where [15, 24]

$$\sigma_{\mathrm{soft}}^{\rho p}(s) \approx \sigma_0 + \sigma_1(s-m_p^2)^{-1/2} + \sigma_2(s-m_p^2)^{-1}. \tag{34}$$

These choices work well in analyses of πp and Kp [16] and $\bar{p}p$ [10, 25] scattering.

B. $q\bar{q}$-proton cross section

We will model the $q\bar{q}$-proton cross section in Eq. (22) using ideas similar to those above, but with changes which reflect the fact that a $q\bar{q}$ system produced at an initial momentum transfer $p_{\perp 0} > Q_0$ does not have time to develop into a system of normal hadronic size. This will be reflected in the $q\bar{q}$-proton overlap function $A_{q\bar{q}\text{-}p}(b)$ which will simply approach $\rho_p(b)$ for a pointlike $q\bar{q}$ system, that is, for $p_{\perp 0} \gg Q_0$. We will parametrize this change by using a form factor for the $q\bar{q}$ system with the same form as G_ρ, Eq. (30), but with μ^2 scaled by a factor $p_{\perp 0}^2/Q_0^2$ as suggested by our earlier discussion:

$$G_{q\bar{q}}(k_\perp^2) = \left(1+\frac{Q_0^2}{4p_{\perp 0}^2}\frac{k_\perp^2}{\mu^2}\right)^{-1}, \qquad p_{\perp 0}^2 \geq \mu^2, \tag{35}$$

where we will take $4Q_0^2 = \mu^2 = 0.47\ (\mathrm{GeV}/c)^2$. The $q\bar{q}$ profile function $\rho_{q\bar{q}}(b)$ and the overlap function $A_{q\bar{q}\text{-}p}(b)$ calculated using the analogues of Eqs. (29) and (27) are then continuous with $\rho_p(b)$ and $A_{\rho p}(b)$ at $p_{\perp 0} = Q_0$, and approach a δ function and $\rho_\rho(b)$, respectively, for $p_{\perp 0} \gg Q_0$.

We must also scale $\sigma_{\mathrm{soft}}(s)$ in Eq. (34) so that the integral of the eikonal function $2\mathrm{Re}\,\chi(b)$ (the intrinsic single-interaction cross section) decreases with the geometrical size of the $q\bar{q}$ system for $p_{\perp 0} > Q_0$. We will simply scale by a factor $(Q_0/p_{\perp 0})^2 = (\mu/2p_{\perp 0})^2$ and take

$$\sigma_{\mathrm{soft}}^{q\bar{q}p} = (\mu^2/4p_{\perp 0}^2)\sigma_{\mathrm{soft}}^{\rho p}. \tag{36}$$

The $q\bar{q}$ and vector-meson terms are then properly continuous at $p_{\perp 0} = Q_0$, while the soft $q\bar{q}$-proton cross section decreases as $1/p_{\perp 0}^2$ for $p_{\perp 0} \gg Q_0$ as is expected for higher-twist contributions [26]. The hard QCD contributions to the eikonal function for the $q\bar{q}$-proton interaction are again of the form given in Eq. (26), but with the parton distributions in the ρ meson replaced by the parton distributions $f_i^{q\bar{q}}(x, p_\perp, p_{\perp 0})$ which evolve from the initial $q\bar{q}$ system produced at the transverse momentum $p_{\perp 0}$ and observed at $p_\perp$.

C. Jet and inclusive cross sections

The inclusive jet cross section $\sigma_{\mathrm{jet}}^{\gamma p}(s, Q^2)$ is defined to be the part of the inelastic γp cross section which includes events with at least one semihard parton-parton scattering with a momentum transfer $p_\perp^2 \geq Q^2$, irrespective of any soft processes which may occur. The semiclassical probability that there is *no* parton-parton scattering with $p_\perp^2 > Q^2$ in a hadronic collision at impact parameter b is $e^{-2\mathrm{Re}\,\chi_{\mathrm{QCD}}(b,s,Q^2)}$. Using this observation, we can rewrite the cross section σ_{inel}^m associated with the hadronic component $|m\rangle$ of the photon as [10, 27, 28]

$$\begin{aligned}\sigma_{\mathrm{inel}}^m &= \int d^2b\left(1-e^{-2\mathrm{Re}\,\chi_{\mathrm{QCD}}^m - 2\mathrm{Re}\,\chi_{\mathrm{soft}}^m}\right)\\ &= \int d^2b\left(1-e^{-2\mathrm{Re}\,\chi_{\mathrm{QCD}}^m(b,s,Q^2)}\right) + \int d^2b\left(1-e^{-2\mathrm{Re}\,\chi'_{\mathrm{soft},\,m}(b,s,Q^2)}\right)e^{-2\mathrm{Re}\,\chi_{\mathrm{QCD}}^m(b,s,Q^2)}\\ &= \sigma_{\mathrm{jet}}^m(s,Q^2) + \sigma_{\mathrm{no\ jet}}^m(s,Q^2)\,.\end{aligned} \tag{37}$$

Here

$$\sigma_{\mathrm{jet}}^m(s,Q^2) = \int d^2b\left(1-e^{-2\mathrm{Re}\chi_{\mathrm{QCD}}^m(b,s,Q^2)}\right) \tag{38}$$

is the total jet cross section. It includes events with multiple independent parton-parton scatterings (multijet events) as well as single-scattering events, all with or without accompanying soft inelastic scattering processes. The eikonal function $\mathrm{Re}\chi_{\mathrm{QCD}}^m(b,s,Q^2)$ is defined as in Eqs. (25) and (26) with $p_{\perp,\mathrm{min}}^2$ replaced by Q^2 in Eq. (26).

$\mathrm{Re}\chi'_{\mathrm{soft},\,m}$ in Eq. (37) includes both the usual soft term and the contributions from jets softer than the (observational) cut imposed, that is, with $p_{\perp,\min}^2 \le p_\perp^2 < Q^2$. It is given by the sum of $\mathrm{Re}\chi_{\mathrm{soft}}^m$ and a modified $\mathrm{Re}\chi_{\mathrm{QCD}}^m$ calculated for the restricted interval $p_{\perp,\min}^2 < p_\perp^2 < Q^2$. The cross section $\sigma_{\text{no jet}}^m$ includes *no* jet events with $p_\perp^2 > Q^2$ as is evident from the probabilistic interpretation of the factor $e^{-2\mathrm{Re}\,\chi_{\mathrm{QCD}}^m}$ in its definition in Eq. (37). The total jet cross section in γp scattering involves direct γ-parton interactions as well, and a generalized sum over the hadronic jet cross sections with the weights $\mathcal{P}_m$:

$$\begin{aligned}\sigma_{\mathrm{jet}}^{\gamma p}(s,Q^2) &= \sigma_{\mathrm{dir}}^{\mathrm{QCD}}(s,Q^2) + \sum_m \mathcal{P}_m \sigma_{\mathrm{jet}}^m(s,Q^2) \\ &= \sigma_{\mathrm{dir}}^{\mathrm{QCD}}(s,Q^2) + \lambda \mathcal{P}_\rho \sigma_{\mathrm{jet}}^\rho(s,Q^2) \\ &\quad + \sum_q e_q^2 \frac{\alpha_{\mathrm{em}}}{\pi} \int_{Q_0^2} \frac{dp_{\perp 0}^2}{p_{\perp 0}^2} \sigma_{\mathrm{jet}}^{q\bar{q}p}(s,Q^2,p_{\perp 0}^2).\end{aligned} \tag{39}$$

To calculate the multijet cross sections, we note that the average number of parton-parton scatterings in a collision at impact parameter b which involves the intermediate hadronic state $|m\rangle$ is

$$\begin{aligned}n_m(b,s,Q^2) &= \sigma_m^{\mathrm{QCD}}(s,Q^2)\, A_m(b) \\ &= 2\mathrm{Re}\,\chi_{\mathrm{QCD}}^m(b,s,Q^2)\ .\end{aligned} \tag{40}$$

Since the parton scatterings in our model are independent, the probability of having n scatterings ($2n$ jets) in a hadronic interaction is given by a Poisson distribution with the average number of scatterings equal to $n_m(b,s,Q^2)$:

$$P_{n,m}(b,s,Q^2) = \frac{1}{n!}\left[n_m(b,s,Q^2)\right]^n e^{-n_m(b,s,Q^2)}\ . \tag{41}$$

The probability distribution for $n = 0, 1, \ldots$ parton scatterings or $2n$ jets with $p_\perp^2 \ge Q^2$ averaged over *all* inelastic events is then given by [10, 28]

$$P_n(s,Q^2) = \frac{1}{\sigma_{\mathrm{inelas}}^{\gamma p}(s)} \sum_m \mathcal{P}_m \frac{1}{n!} \int d^2b \left[n_m(b,s,Q^2)\right]^n e^{-n_m(b,s,Q^2)}, \quad n \ge 1, \tag{42}$$

$$P_0(s,Q^2) = \frac{1}{\sigma_{\mathrm{inelas}}^{\gamma p}(s)} \sum_m \mathcal{P}_m \int d^2b \left(1 - e^{-2\mathrm{Re}\,\chi'_{\mathrm{soft},\,m}(b,s,Q^2)}\right) e^{-n_m(b,s,Q^2)}. \tag{43}$$

The sum in Eq. (42) just gives $\sigma_{\mathrm{jet}}^{\gamma p}$ up to the very small single-jet contribution from the direct-interaction cross section in Eq. (39). We note that the factors $e^{-n(b,s,Q^2)}$ and $(1 - e^{-2\mathrm{Re}\chi'_{\mathrm{soft}}})$ in the expression for P_0 are simply interpreted as the Poisson probability that there are no hard parton-parton scatterings, and the probability that there *is* a soft inelastic interaction in the hadronic collision in question.

We note finally that the average number of parton-parton collisions with $p_\perp^2 > Q^2$ is given by

$$\bar{n}(s,Q^2) = \sum_{n=1}^{\infty} n P_n(s,Q^2). \tag{44}$$

Using the results above and the normalization condition for the overlap function $A(b)$ in Eq. (27), Eq. (44) is easily shown to reduce to the statement that

$$\begin{aligned}\bar{n}\sigma_{\mathrm{inelas}}^{\gamma p} &= \sum_m \mathcal{P}_m \sigma_{\mathrm{QCD}}^m(s,Q^2) \\ &= \sum_{i,j} \int_0^1 dx_1 \int_0^1 dx_2 \int_{Q^2} dp_\perp^2 f_i^p(x_1,p_\perp^2) \frac{d\hat{\sigma}_{ij}}{dp_\perp^2} \\ &\quad \times \sum_m \mathcal{P}_m f_j^m(x_2,p_\perp^2),\end{aligned} \tag{45}$$

where the factors $\mathcal{P}_m$ are again the probabilities with which the hadronic states $|m\rangle$ appear in the photon. This is just the usual expression for the inclusive hadronic γp cross section,

$$\bar{n}\sigma_{\mathrm{inelas}}^{\gamma p} = \sum_{i,j} \int_0^1 dx_1 \int_0^1 dx_2 \int_{Q^2} dp_\perp^2 f_i^p(x_1,p_\perp^2) \frac{d\hat{\sigma}_{ij}}{dp_\perp^2} \times f_j^\gamma(x_2,p_\perp^2), \tag{46}$$

but with the photon structure functions given explicitly as weighted sums over the structure functions for the initial hadronic components of the photon, that is, with

$$\begin{aligned}f_i^\gamma(x,p_\perp^2) &= \sum_m \mathcal{P}_m f_i^m(x,p_\perp^2) \\ &\approx \lambda \mathcal{P}_\rho f_i^\rho(x,p_\perp^2) \\ &\quad + \sum_q e_q^2 \frac{\alpha_{\mathrm{em}}}{\pi} \int_{Q_0^2}^{p_\perp^2} \frac{dp_{\perp 0}^2}{p_{\perp 0}^2} f_i^{q\bar{q}}(x,p_\perp^2,p_{\perp 0}^2).\end{aligned} \tag{47}$$

This is just what would be expected for f_i^γ in the standard semiclassical picture of the parton model.

D. Parton distributions in the hadronic photon

The remaining problem is the specification of the parton distributions for the ρ meson and the $q\bar{q}$ system which appear in the expression for $\mathrm{Re}\,\chi_{\mathrm{QCD}}$. There are no direct measurements of these quantities. We have considered two approaches to the problem. In the first, we use the equivalence of the ρ and π states in the quark model up to spin effects to equate the distribution functions f_i^ρ to the corresponding distribution functions f_i^π

for the pion. This is a generalization of a standard approximation in the vector-dominance model for photon-hadron interactions [29], and is a commonly used starting point in the treatment of the photon distribution functions [30–32]. Although the distribution functions for the pion [33] are not known as well as those for the proton, they have been tested in an analysis of high-energy $\pi^{\pm}p$ scattering [16] which involved the same QCD effects as are important here, and seem to be satisfactory.

An alternative approach is to try to relate f_i^{ρ} and $f_i^{q\bar{q}}$ to f_i^{γ} using a model to invert Eq. (47) approximately. (The eikonal functions cannot be expressed directly in terms of f_i^{γ} as is evident from a comparison of Eqs. (22) and (47)— see also [20].) The approximation used in earlier work [9, 11, 12] was to equate f_i^{ρ} to the corresponding distribution function for the photon, with the probability that the photon becomes a ρ meson divided out. This gives the estimate

$$f_i^{\rho} \approx f_i^{\gamma}/\mathcal{P}_{\rho}. \tag{48}$$

This estimate does not include the contributions to f_i^{γ} in Eq. (47) from vector mesons other than the ρ, or those from the excited $q\bar{q}$ hadronic states produced at initial momentum transfers $Q_0 < p_{\perp 0} < p_{\perp}$, both of which are significant.

The contributions from the excited vector states are expected to fall as $1/p_{\perp 0}^2$. We will estimate these contributions by assuming that

$$f_i^{q\bar{q}}(x, p_{\perp}^2, p_{\perp 0}^2) \approx \left(\frac{Q_0}{p_{\perp 0}}\right)^2 f_i^{\rho}(x, p_{\perp}^2) \tag{49}$$

for $p_{\perp} > p_{\perp 0} > Q_0$, thus enforcing continuity in the distributions, and integrating Eq. (47). The result, which is properly independent of Q_0 for $p_{\perp} \gg Q_0$, is given for three light quarks by

$$f_i^{\gamma} \approx \left(\lambda \mathcal{P}_{\rho} + \frac{2}{3}\frac{\alpha_{\rm em}}{\pi}\right) f_i^{\rho}. \tag{50}$$

The effect is to replace $\mathcal{P}_{\rho}$ in Eq. (48) by

$$\mathcal{P}' = \lambda \mathcal{P}_{\rho}\left(1 + \frac{2}{3\pi\lambda}\frac{f_{\rho}^2}{4\pi}\right). \tag{51}$$

Numerically, $\mathcal{P}' \approx 1.8\mathcal{P}_{\rho}$ for $f_{\rho}^2/4\pi = 2.2$ and $\lambda = 4/3$ (equal Vp cross sections for the ρ, ω, and ϕ mesons), and $\mathcal{P}' \approx 1.58\mathcal{P}_{\rho}$ for $\lambda = 10/9$ (complete suppression of the ϕ contribution). The last factor in Eq. (51), which accounts for the contributions of the excited states to f^{γ}, is equal to 1.35 for $\lambda = 4/3$, a value which agrees well with estimates in vector-dominance models [29].

The approximation for f_i^{γ} in Eq. (50) neglects any dependence of $f_i^{q\bar{q}}$ on $p_{\perp 0}$ other than that in the scaling factor, for example, the effect of the different ranges of QCD evolution from $p_{\perp 0}$ to $p_{\perp}$ for systems produced at different $p_{\perp 0}$. It simply equates f_i^{γ} to a multiple of f_i^{ρ} as in simple vector-dominance arguments [29], with $\mathcal{P}'$ determined to make Eq. (47) an identity within the approximation used.

Additional purely perturbative contributions to the f_i^{γ} are generated by the inhomogeneous term in the QCD evolution equations for the quark distributions in the photon [34]:

$$\frac{dq_i^{\gamma}}{d\ln(Q^2/\Lambda^2)}(x,Q^2) = 3e_i^2\frac{\alpha_{\rm em}}{2\pi}\left[x^2+(1-x)^2\right] + \frac{\alpha_s}{2\pi}(Q^2)\int_x^1 \frac{dy}{y}\left[P_{qq}\left(\frac{x}{y}\right)q_i^{\gamma}(y,Q^2) + P_{qG}\left(\frac{x}{y}\right)G^{\gamma}(y,Q^2)\right],$$

$$\frac{dG^{\gamma}}{d\ln(Q^2/\Lambda^2)}(x,Q^2) = \frac{\alpha_s(Q^2)}{2\pi}\int_x^1 \frac{dy}{y}\left[\sum_{i=1}^{2f} P_{Gq}\left(\frac{x}{y}\right)q_i^{\gamma}(y,Q^2) + P_{GG}\left(\frac{x}{y}\right)G^{\gamma}(y,Q^2)\right], \tag{52}$$

where the P's are the usual quark and gluon splitting functions. Forshaw [20] estimated these "pointlike" contributions starting with vanishing distribution functions at $p_{\perp 0} = 1$ GeV, and found them to be small at the momentum transfers $p_{\perp}$ which are relevant for our considerations.

Finally, for either of the foregoing models for f_i^{ρ}, we can estimate $f_i^{q\bar{q}}(x, p_{\perp}^2, p_{\perp 0}^2)$ simply as $(Q_0/p_{\perp 0})^2 f_i^{\rho}(x, p_{\perp}^2)$. This estimate assumes that the initial nonperturbative parton distributions $f_i^{q\bar{q}}$ at $p_{\perp 0} > Q_0$ can be equated to the ρ-meson distributions at $p_{\perp 0}$ scaled by the size of the system, with the distribution then evolved to $p_{\perp}$ using the homogeneous part of the QCD evolution equations (the evolution equations for the ρ or π do not have an inhomogeneous term). The final distributions therefore include the effects of evolution all the way from Q_0 to $p_{\perp}$. A better treatment would use the scaled distributions at Q_0 as input for evolution from $p_{\perp 0}$ to $p_{\perp}$, again using the homogeneous version of the evolution equations. This calculation may become worthwhile in the future, but we do not expect the differences from the present estimates to be large since large values of $p_{\perp}$ and $p_{\perp 0}$ are suppressed by the rapid decrease in the parton-level cross sections and the $(Q_0/p_{\perp 0})^2$ scaling, respectively.

To summarize, the total inelastic γp cross section is given by

$$\sigma_{\rm inel}^{\gamma p} = \sigma_{\rm dir} + 2\lambda\mathcal{P}_{\rho}\int d^2b\left(1 - e^{-{\rm Re}\,\chi_{\rho p}}\right) + \sum_q 2e_q^2\frac{\alpha_{\rm em}}{\pi}\int_{Q_0^2}\frac{dp_{\perp 0}^2}{p_{\perp 0}^2}\int d^2b\left(1 - e^{-{\rm Re}\,\chi_{q\bar{q}p}}\right). \tag{53}$$

Here

$$2\mathrm{Re}\,\chi_{\rho p}(b,s) = A_{\rho p}(b)\left[\sigma_{\mathrm{soft}}(s) + \sigma_{\mathrm{QCD}}^{\rho p}(s)\right], \quad (54)$$

where $A_{\rho p}$, $\sigma_{\mathrm{soft}}^{\rho p}$, and $\sigma_{\mathrm{QCD}}^{\rho p}$ are given in Eqs. (32), (34), and (26), respectively. Finally,

$$2\mathrm{Re}\,\chi_{q\bar{q}p}(b,s,p_{\perp 0})$$

$$= A_{q\bar{q}p}(b,p_{\perp 0})\left[\sigma_{\mathrm{soft}}^{q\bar{q}p}(s,p_{\perp 0}) + \sigma_{\mathrm{QCD}}^{q\bar{q}p}(s,p_{\perp 0})\right], \quad (55)$$

where $A_{q\bar{q}p}$ is given by Eq. (32) with μ replaced by $2p_{\perp 0}$, $\sigma_{\mathrm{soft}}^{q\bar{q}p}$ is given by Eq. (36), and $\sigma_{\mathrm{QCD}}^{q\bar{q}p}$ is given by the analogue of Eq. (26) with f_i^{ρ} replaced by $f_i^{q\bar{q}} \approx (Q_0/p_{\perp 0})^2 f_i^{\rho}$.

The results above differ from those in earlier work in important ways. Thus the authors of [9], [11], and [12] omit the last term in Eq. (53), estimate the ρ-meson structure functions f_i^{ρ} in $\chi_{\rho p}$ using the approximation in Eq. (48), and ignore contributions other than those of the ρ, i.e., take $\lambda = 1$ in Eq. (53). Forshaw's recent analysis [20] includes the last term in Eq. (53), but with $\chi_{q\bar{q}p}$ restricted to the purely "pointlike" contributions which he shows are small. His discussion neglects the residual soft contributions from excited states. These fall as $1/p_{\perp 0}^2$ in our model as expected for "higher-twist" contributions, but are nevertheless important. The last term contributes approximately 1/3 of the cross section at the energies of interest in our applications. The direct cross section is quite small, roughly 1.5% of the total at HERA energies. We reemphasize, finally, that continuity in the expressions at $p_{\perp 0} = Q_0$ is essential since "hard" and "soft" processes are not clearly separated and must merge smoothly.

IV. RESULTS FOR THE γp AND γ-NUCLEUS CROSS SECTIONS

A. γp cross sections

Our calculations of the inelastic γp cross sections were based on Eq. (53), with the eikonal functions parametrized as described earlier. We note, in particular, that our Regge-type parametrization of σ_{soft} allows us to connect the high- and low-energy cross sections smoothly. Previous calculations [3,6,11,12] have taken σ_{soft} as constant, with the value chosen to fit the measured γp cross section near its minimum at $\sqrt{s} \approx 8$ GeV, and fail at lower energies. The (eikonalized) soft cross section in the "high-energy" range 7 GeV $\leq \sqrt{s} \leq$ 20 GeV actually involves a significant contribution from the decreasing terms in Eq. (34) which are necessary to fit the lower-energy data. This affects the value of $p_{\perp,\mathrm{min}}$ needed to fit these data using the rising QCD contributions and, hence, affects the increase in the cross section predicted at high energies. We obtain quite reasonable fits to the data for 3 GeV $\leq$ 10 GeV [35] using the soft cross section in Eq. (34), but have not tried to obtain a "best" fit given the apparent inconsistencies in normalization between different experiments.

The cross section $\sigma_{\mathrm{had}}^{\mathrm{QCD}}$ for semihard scattering was calculated using the exact formulas for the $O(\alpha_s^2)$ parton-parton cross sections. The strong coupling $\alpha_s(Q^2)$ was evaluated at the scale $Q^2 = p_{\perp}^2$ for four flavors with $\Lambda_{\mathrm{QCD}} = 200$ MeV. We used the proton structure functions of Eichten *et al.* [36,37]. The results do not change significantly [6] for different parametrizations [21] of the proton structure functions. For the two models we considered for the ρ-meson and $q\bar{q}$ structure functions, we used the pion structure functions of Owens [33] and the photon structure functions of Drees and Grassie [31]. The photon structure functions of Duke and Owens [38] give very similar results in the region $\sqrt{s} \lesssim 20$ GeV in which there are data, but are unrealistically singular for $x \to 0$, and are not reliable for high-energy applications [6]. The direct cross section in Eq. (7) was also calculated using the proton structure functions of Eichten *et al.* [36], and the same value of $p_{\perp,\mathrm{min}}$ as used in the hadronic terms. The direct cross section is always very small relative to the hadronic cross section.

For the model based on the pion structure functions, we used the value $p_{\perp,\mathrm{min}} = 1.45$ GeV which was fixed in earlier fits to the πp scattering cross sections [16]. The results are essentially independent of Q_0 provided $p_{\perp,\mathrm{min}}^2 \gg Q_0^2$, a condition which is satisfied for $Q_0^2 \approx \mu^2/4 \approx 0.12$ GeV^2 [39]. The only adjustable parameters are then the three cross sections $\sigma_0, \sigma_1, \sigma_2$ which appear in the soft cross section in Eq. (34), and the parameter λ which specifies the extent to which the ϕ meson contributes to the sum of cross sections in Eq. (10). The parameter σ_2 is important only at very low energies. The remaining parameters are reasonably well fixed by the data between $\sqrt{s} = 3$ GeV and $\sqrt{s} = 20$ GeV once λ is specified. The parameters used for the two cases considered, $\lambda = 4/3$ (no ϕ suppression) and $\lambda = 10/9$ (complete ϕ suppression) are listed in Table I.

The calculated cross sections are compared to the data below $\sqrt{s} = 20$ GeV in Fig. 1, which shows how the use of a Reggeized soft cross section gives a smooth connection between the low-energy region 3 GeV $\leq \sqrt{s} \leq 10$ GeV and the high-energy region 10 GeV $\leq \sqrt{s} \leq 20$ GeV. The effects of semihard parton scatterings begin to be important in the latter region, and account for the observed increase in the inelastic γp scattering cross section. We have not attempted to fit the cross-section data below $\sqrt{s} = 2$ GeV ($E_{\gamma,\mathrm{lab}} = 1.66$ GeV) where resonance effects become important.

We show the results for the region 3 GeV $\leq \sqrt{s} \leq 20$ GeV in more detail in Fig. 2. This figure clearly shows the increase in $\sigma_{\mathrm{inel}}^{\gamma p}$ associated with the onset of semihard parton scatterings. It shows also the importance of including the lower-energy region in the analysis: The observed rise in the cross section is relative to a falling contribution from soft processes in this energy region. This "background" is shown in Fig. 2 as the curve for the eikonalized soft cross section calculated including the soft contributions from the last two terms in Eq. (53), plus the very small contribution from the direct cross section. The two cases considered, $\lambda = 4/3$ and $\lambda = 10/9$, give results for this background which are practically indistinguishable even though the soft backgrounds are somewhat different.

The ρp cross section can be calculated using Eq. (23),

TABLE I. Values of the parameters used in the calculations shown in Figs. 1–5.

	σ_0 (mb)	σ_1 (mb GeV)	σ_2 (mb GeV^2)
ϕ suppressed	22.3	15.0	5.0
ϕ included	19.2	13.1	3.9

the soft backgrounds determined above, and the pion distribution functions in the QCD contribution to the eikonal function. The results are rather close to the measured $\pi^{\pm}p$ cross sections in this energy range as would be expected in a model which treats the ρ and π as equivalent. In particular, the calculated ρp cross section is about 11% lower than the average of the $\pi^{\pm}p$ cross sections at $\sqrt{s} = 10$ GeV when calculated using the soft background determined for $\lambda = 10/9$, and about 21% low when calculated using the soft background for $\lambda = 4/3$. The two cases bracket the measured ρp cross sections which are about 15% below the $\pi^{\pm}p$ cross section [15].

The cross sections predicted for the two cases diverge mildly at higher energies as shown in Fig. 3. The divergence is primarily due to the suppression of the ϕ contribution for $\lambda = 10/9$. The soft background in the two cases differs by less than 0.001 mb at $\sqrt{s} = 400$ GeV. A curve close to the lower curve with $\lambda = 10/9$ is probably to be preferred since the data on photoproduction for $\sqrt{s} \approx 10$ GeV show strong suppression of the measured ϕ-to-ρ^0 production ratio relative to that expected in the vector-dominance model with quark-model couplings [17, 40]. We also illustrate the effects of the eikonalization procedure in Fig. 3 by including the result obtained by simply adding the inclusive QCD cross section for γp scattering to the eikonalized soft background, a procedure followed in early theoretical estimates and the comparisons with data given in [14]. The effects are substantial.

As shown in Fig. 3 the predictions for $\sigma^{\gamma p}_{\rm inel}$ based on the pion structure functions are somewhat higher than, but consistent with, the preliminary measurements at HERA reported by the ZEUS and H1 Collaborations [14]. Since the main contribution to $\sigma_{\rm QCD}$ at high energies arises from the scattering of low-x gluons, a high value of the calculated cross section would suggest that the gluon content of the pion had been overestimated in [33]. The approximate photon structure functions given by the expression in Eqs. (47) and (50) with f_i^{ρ} equated to f_i^{π} would then have a gluon content which is also somewhat too large at low x.

Our results for the model based on the photon structure functions of Drees and Grassie [31] with the factor $\mathcal{P}'$ in Eq. (51) divided out are shown in Figs. 4 and 5. The curves shown in these figures were calculated using $p_{\perp,\rm min} = 1.2$ GeV and 1.4 GeV and the soft parameters given in Table I. It was assumed that the ϕ contribution is suppressed. If it is not, the curves shown would be higher at $\sqrt{s}$=200 (400) GeV by 9 (15) μb and 7 (11) μb for $p_{\perp,\rm min}$=1.2 and 1.4 GeV, respectively. The curves shown in Fig. 4 bracket the data for 6 GeV $\leq \sqrt{s} \leq 20$ GeV. An intermediate value of the QCD cutoff, $p_{\perp,\rm min} \approx 1.3$ GeV, is clearly favored. The results

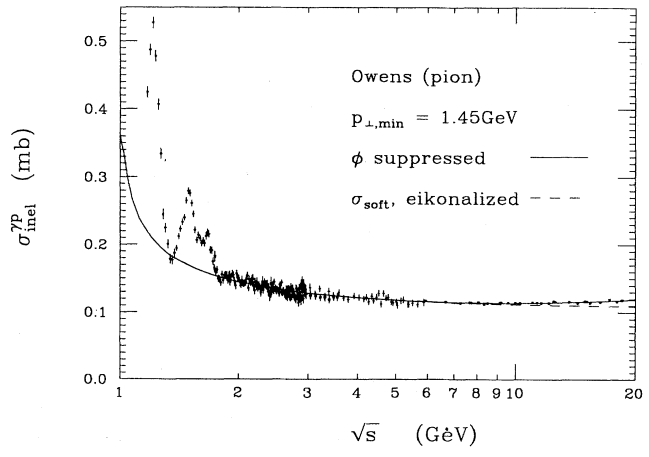

FIG. 1. Inelastic γp scattering cross section for $\sqrt{s} \leq 20$ GeV predicted by the model in the text using pion structure functions. The data are from the references in [35]. The soft contributions to the cross section were determined using data for 3 GeV $\leq \sqrt{s} \leq 8$ GeV only. The QCD contributions were calculated using $p_{\perp,\rm min} = 1.45$ GeV, the value determined in [16] in a fit to $\pi^{\pm}p$ cross sections for 10 GeV $\leq \sqrt{s} \leq 26$ GeV.

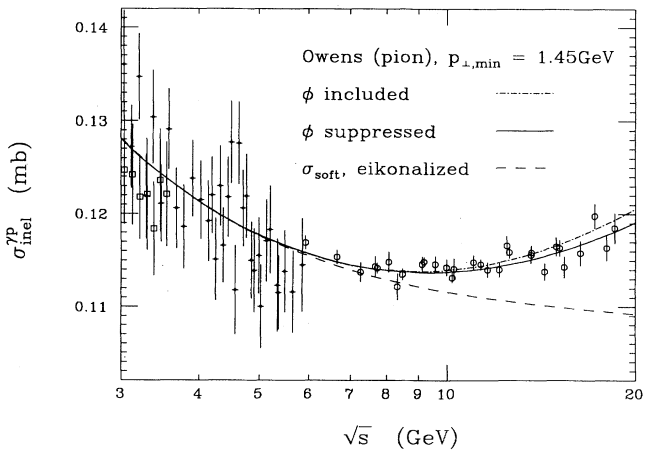

FIG. 2. Inelastic γp cross section for 3 GeV $\leq \sqrt{s} \leq 20$ GeV compared to the cross sections predicted using pion structure functions, with the ϕ-meson contribution at full strength or totally suppressed. The data shown are from [35].

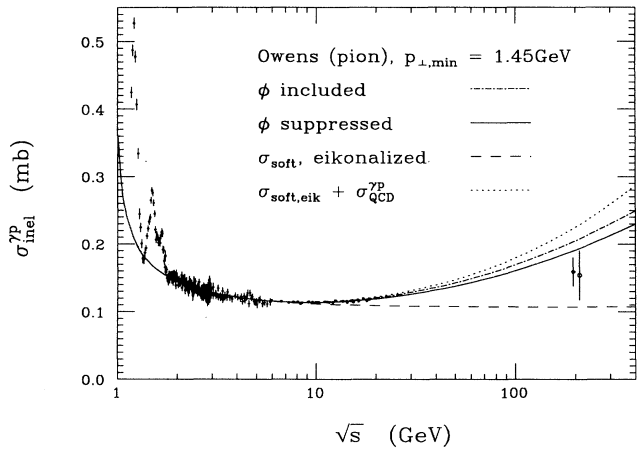

FIG. 3. Predictions for $\sigma^{\gamma p}_{\rm inel}$ for $\sqrt{s} \leq 400$ GeV for the model based on pion structure functions with the ϕ-meson contribution present or totally suppressed. The lower-energy data are from [35]. The preliminary HERA data at $\sqrt{s} \approx 200$ GeV are from [14].

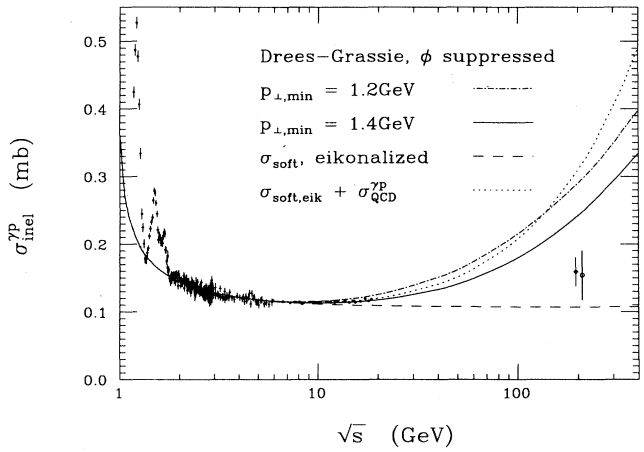

FIG. 5. Predictions for $\sigma^{\gamma p}_{\rm inel}$ for $\sqrt{s} \leq 400$ GeV for the model base on the Drees-Grassie structure functions for the photon with $p_{\perp,\rm min} = 1.2$ GeV and 1.4 GeV, and complete suppression of the ϕ-meson contribution. The lower-energy data are from [35]. The preliminary HERA data at $\sqrt{s} \approx 200$ GeV are from [14].

obtained at higher energies with the Drees-Grassie structure functions are shown in Fig. 5. The calculated cross sections are significantly higher than those obtained using the pion structure functions, and rise more rapidly at high energies. The predictions at $\sqrt{s} = 200$ GeV are clearly inconsistent with the preliminary measurements of $\sigma^{\gamma p}_{\rm inel}$ at HERA [14]. The very rapid rise in the calculated cross sections for $\sqrt{s} \gtrsim 200$ GeV is associated with the rapid growth of the parton distribution functions at the small values of x which become accessible at these energies. The difficulty is also evident in the cross-section curve for the additive model which rises much more rapidly than the corresponding curve in Fig. 3.

The cutoff $p_{\perp,\rm min}$ would have to be increased to roughly 1.7 GeV to bring the calculated high-energy cross section to the same level of agreement with the HERA data as was obtained with the pion distribution functions in Fig. 3. However, a value of $p_{\perp,\rm min}$ that large would be inconsistent with the data for $\sqrt{s} < 20$ GeV as shown by Fig. 4. In particular, the increase in the QCD-enhanced cross section relative to the soft background is less than 2.5 μb over the interval 8 GeV $< \sqrt{s} <$ 20 GeV for $p_{\perp,\rm min}$= 1.7 GeV. This is not sufficient to account for the observed increase even for a flat background, that is, ignoring the clear energy dependence of the lower-energy data. It would therefore be necessary at the least to include a rising (Regge-like) term in the soft cross section to fit the data in the interval above. While we would

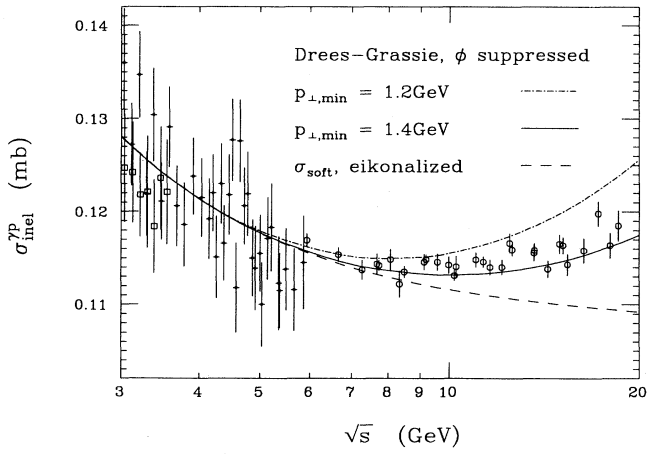

FIG. 4. Inelastic γp cross sections for 3 GeV $\leq \sqrt{s} \leq 20$ GeV compared to the cross sections predicted using the Drees-Grassie structure functions for the photon with $p_{\perp,\rm min} = 1.2$ GeV and 1.4 GeV and complete suppression of the ϕ-meson contribution. The data are from [35].

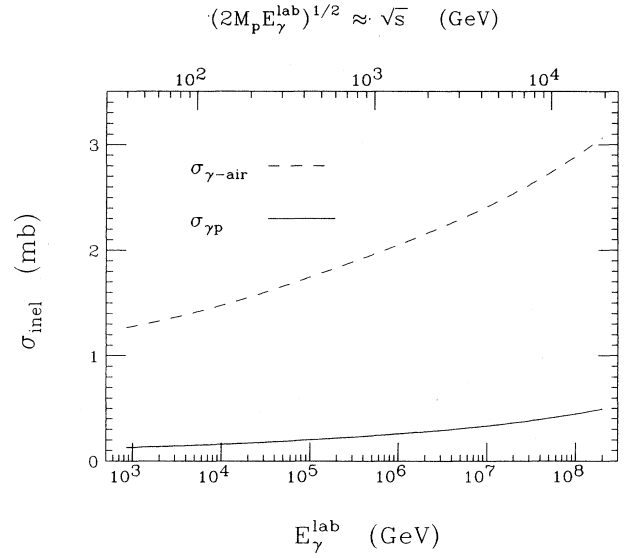

FIG. 6. Predictions for $\sigma^{\gamma p}_{\rm inel}$ and $\sigma^{\gamma\text{-air}}_{\rm inel}$ for $\sqrt{s} \leq 2 \times 10^4$ GeV or $E_{\gamma,\rm lab} \leq 2 \times 10^8$ GeV for the model based on pion structure functions.

then most likely be able to fit the HERA cross sections as well, the modified model would not *predict* those cross sections unless the new parameters could be determined elsewhere. We have therefore not investigated models of this type in detail [41].

B. γ-air cross sections

Our model for the hadronic interactions of the photon can be extended to photon-nucleus interactions using Glauber's multiple-scattering theory [42] with the result

$$\sigma_{\rm inel}^{\gamma\text{-air}} = A\sigma_{\rm dir} + 2\lambda\mathcal{P}_\rho \int d^2b \left\langle \Psi \left| 1 - \exp\left(- \sum\nolimits_{j=1}^{A} {\rm Re}\,\chi_j^{\rho p} \right) \right| \Psi \right\rangle + \sum_q 2e_q^2 \frac{\alpha_{\rm em}}{\pi} \int_{Q_0^2} \frac{dp_{\perp 0}^2}{p_{\perp 0}^2} \int d^2b \left\langle \Psi \left| 1 - \exp\left(- \sum\nolimits_{j=1}^{A} {\rm Re}\chi_j^{q\bar{q}p} \right) \right| \Psi \right\rangle . \quad (56)$$

The expectation values are to be taken in the nuclear ground state. ${\rm Re}\chi_j^m = {\rm Re}\chi^m(|\mathbf{b} - \mathbf{r}_{j\perp}|)$ is the eikonal function for the scattering of the hadronic component $|m\rangle$ of the photon on the jth nucleon, where $\mathbf{r}_{j\perp}$ is the instantaneous transverse distance of that nucleon from the nuclear center of mass, and $\mathbf{b}$ is the impact parameter of the photon relative to the nucleus. The integrals were evaluated using shell-model wave functions for the oxygen and nitrogen nuclei [43]. The eikonal functions for γn and γp scattering were taken as equal.

In Fig. 6 we show the inelastic γp cross section for laboratory photon energies up to 2×10^8 GeV ($\sqrt{s} \approx 2 \times 10^4$ GeV), calculated as described above using the parton distribution functions of Eichten *et al.* [36] for the proton and the pion structure functions of Owens [33] for the photon with the ϕ contribution suppressed. The eikonalized γp cross section rises to 0.5 mb at $E_{\gamma,\rm lab} = 2 \times 10^8$ GeV, a large value for a photon-initiated process, but still a small cross section on a hadronic scale. Since the results obtained in [16] for πp scattering at equivalent energies suggest that the gluon content of the pion given by [33] is too large, the γp cross section shown in Fig. 6 should be regarded as an upper limit. A generous upper bound on the γ-air cross section is given by $A\sigma_{\rm inel}^{\gamma p}$, which reaches 7.2 mb for $E_{\gamma,\rm lab} = 2 \times 10^8$ GeV, and $A_{\rm air} \approx 14.4$. The actual cross section is lower, as shown in Fig. 6, reaching only 3 mb at $E_{\gamma,\rm lab} = 2 \times 10^8$ GeV. The limit is far below the result $\sigma_{\rm inel}^{\gamma p} \approx 90$ mb obtained in [6] using the incorrect eikonalization procedure noted in the Introduction, and is clearly far too small to account for the reported muon anomalies in cosmic-ray air showers. The γ-air cross section may still be large enough to be interesting for shower evolution.

C. Conclusions and comments

Our main conclusion is simple: The proper treatment of eikonalization in the calculation of inelastic γp interactions is important even at rather low energies. This is clearly seen in Figs. 3 and 5, and is in accord with the observations of Collins and Ladinsky [9]. However, the situation is somewhat more complex than envisaged by those authors. The γp cross section is given as a weighted sum of cross sections for the different hadronic components of the photon, and cannot be expressed directly in terms of the photon structure functions.

We have formulated a simple model which includes contributions to the cross section from the low-mass vector mesons and from excited states described in a quark-gluon basis. The soft cross sections and quark and gluon distributions for the excited states are taken as scaled versions of the corresponding quantities for the ρ meson, and the distribution functions for the ρ are equated to those for the pion. The model works well at lower energies using the cutoff $p_{\perp,\rm min}$ in the QCD contributions which was determined for πp scattering in [16], and gives a reasonable but perhaps somewhat high cross section at the energy of the preliminary measurements at HERA, $\sqrt{s} \approx 200$ GeV [14]. The discrepancy, if real [44], suggests that the gluon content of the pion has been overestimated at small x in [33], a conclusion consistent with that in [16].

We emphasize that our result at $\sqrt{s} = 200$ GeV is a genuine prediction within our picture of the γp interaction. The parametrization of the low-energy cross section is essentially independent of the very small QCD contributions in that energy range, and gives results for the ρp cross section which agree with observation [15]. The only remaining parameter, $p_{\perp,\rm min}$, was fixed from the πN scattering data, and was *not* adjusted to fit either the rise in $\sigma^{\gamma p}$ observed for 8 GeV $\lesssim \sqrt{s} \lesssim$ 20 GeV or the HERA data. The πp and γp cross sections are therefore tied together in a consistent picture which appears to be rather stable. The soft backgrounds were quite similar in the two cases and the same parton distributions were used, and so a change in one of the components, for example, the parton distributions, must be compensated by similar changes in the other component in *both* πp and γp scattering. The two cannot be treated as independent.

The model also gives an interesting *a priori* estimate for the quark and gluon distributions in the photon valid at momentum transfers at which the pointlike components of the photon are unimportant [20]:

$$f_i^\gamma = \lambda \frac{4\pi\alpha_{\rm em}}{f_\rho^2} \left(1 + \frac{2}{3\pi\lambda} \frac{f_\rho^2}{4\pi} \right) f_i^\pi , \quad (57)$$

where $10/9 < \lambda < 4/3$. It will be interesting to compare future direct measurements of f_i^γ at HERA with this estimate using the pion structure functions of Owens [33] which are successful in the present application.

The version of the model in which the ρ distribution

functions are estimated from the photon structure functions f_i^γ of Drees and Grassie gives high-energy cross sections which are too large to agree with the new HERA data [14] if the observed rise in the data for 8 GeV $\leq \sqrt{s} \leq 20$ GeV is attributed entirely to a QCD contribution which rises relative to a falling soft background. We have not checked other sets of photon structure functions directly. However, recent calculations by Forshaw and Storrow [45], using the photon distribution functions of Glück, Reya, and Vögt [32] and Abramowicz, Charchula, and Levy [46], give larger values of $\sigma_{\rm QCD}^{\gamma p}$ at $\sqrt{s} = 200$ GeV than those obtained with the Drees-Grassie distribution functions [31], and so a change to those f^γ's would not improve the fits. It may well be possible to fit both the low-energy and the HERA data by including a rising Regge-like term in the soft background, but the model then loses predictive power unless that contribution and the parameter $p_{\perp,\rm min}$ can be determined independently of the high-energy data [41].

Finally, extrapolation of $\sigma_{\rm inelas}^{\gamma p}$ and $\sigma_{\rm inelas}^{\gamma\text{-air}}$ to the highest cosmic-ray energies gives cross sections of a few millibarns, large enough to be interesting, but much too small to account for the reported muon anomalies in photon-initiated air showers. The ultrahigh-energy cross sections are of course very uncertain because of our lack of detailed knowledge of the small-x behavior of the parton distributions in the ρ meson and nucleon, but the effects of proper eikonalization are strong enough that much larger cross sections would appear to be precluded.

ACKNOWLEDGMENTS

This work was supported in part through U.S. Department of Energy Grants Nos. DE-AC02-76ER00881 and DE-FG02-85ER40213, and in part by the World Laboratory. One of the authors (L.D.) would like to thank Dr. J. R. Forshaw for useful correspondence, and the Aspen Center for Physics for its hospitality while parts of this work were done.

[1] M. Drees and R.M. Godbole, Phys. Rev. Lett. **61**, 682 (1988); Phys. Rev. D **39**, 169 (1989).

[2] H. Baer, J. Ohnemus, and J. Owens, Z. Phys. C **42**, 659 (1989); R.S. Fletcher, F. Halzen, and R. Robinett, Phys. Lett. B **225**, 176 (1989); R.S. Fletcher, F. Halzen, S. Keller, and W.H. Smith, University of Wisconsin Report No. MAD/PH/633 (unpublished).

[3] R. Gandhi and I. Sarcevic, Phys. Rev. D **44**, R10 (1991).

[4] M. Drees and F. Halzen, Phys. Rev. Lett. **61**, 275 (1988).

[5] M. Drees, F. Halzen, and K. Hikasa, Phys. Rev. D **39**, 1310 (1989).

[6] R. Gandhi, I. Sarcevic, A. Burrows, L. Durand, and H. Pi, Phys. Rev. D **42**, 263 (1990).

[7] T.K. Gaisser, F. Halzen, T. Stanev, and E. Zas, Phys. Lett. B **243**, 444 (1990).

[8] M. Samorski and W. Stamm, Astrophys. J. **17**, L268 (1983); B.L. Dingus *et al.*, Phys. Rev. Lett. **61**, 1906 (1988); S. Sinha *et al.*, Tata Institute of Fundamental Research Report No. OG 4.6-23 (unpublished); V.V. Alexeenko *et al.*, presented at the III VHE Gamma Ray Astronomy Workshop, Crimea, U.S.S.R. (unpublished).

[9] J.C. Collins and G.A. Ladinsky, Phys. Rev. D **43**, 2847 (1991).

[10] L. Durand and H. Pi, Phys. Rev. Lett. **58**, 303 (1987); Phys. Rev. D **38**, 78 (1988); **40**, 1436 (1989); in *Elastic and Diffractive Scatterings*, Proceedings of the Workshop, Evanston, Illinois, 1989, edited by M.M. Block and A.R. White [Nucl. Phys. B (Proc. Suppl.) **12**, 379 (1990)].

[11] R.S. Fletcher, T.K. Gaisser, and F. Halzen, Phys. Rev. D **45**, 377 (1992); **45**, 3279(E) (1992).

[12] J.R. Forshaw and J.K. Storrow, Phys. Lett. B **268**, 116 (1991).

[13] We would like to thank J.R. Forshaw for pointing out an important error in our first approach to this extended calculation.

[14] The preliminary values of $\sigma_{\rm inel}^{\gamma p}$ are the following: ZEUS Collaboration, Phys. Lett. B **293**, 465 (1992), $\sigma^{\gamma p} = 154 \pm 16 \pm 32$ μb at an average energy $\sqrt{s} = 210$ GeV; H1 Collaboration, *ibid.* **299**, 374 (1993), $\sigma_{\gamma p} = 159 \pm 7 \pm 20$ μb at $\sqrt{s} = 195$ GeV.

[15] See, for example, the review by T.H. Bauer, R.D. Spital, D.R. Yennie, and F.M. Pipkin, Rev. Mod. Phys. **50**, 261 (1978).

[16] L. Durand and H. Pi, Phys. Rev. D **43**, 2125 (1991).

[17] The ratio of the cross section $\gamma p \to \phi p$ to that for $\gamma p \to \rho^0 p$ is smaller for $\sqrt{s} = 10$ GeV by a factor of about 0.3 than would be expected for equal ϕp and $\rho^0 p$ elastic scattering cross sections and the quark model ratio 2/9 for the ratio of the ϕ to ρ^0 couplings to the photon. See R.M. Egloff *et al.*, Phys. Rev. Lett. **43**, 657 (1979).

[18] The approximate equivalence of the π and ρ mesons, up to spin effects, is familiar in the quark model, and is supported in the context of scattering processes by the near equality of the measured πp and ρp cross sections [15].

[19] C.J. Bebek, C.N. Brown, M. Herzlinger, S.D. Holmes, C.A. Lichtenstein, F.M. Pipkin, S. Raither, and L.K. Sisterson, Phys. Rev. D **13**, 25 (1976); E. Amaldi, S. Fubini, and G. Furlan, *Pion Electroproduction* (Springer, New York, 1979), Secs. 2.21 and 5.2.

[20] The separation of the soft and pointlike components of the hadronic photon using a momentum-transfer cutoff has been discussed in the context of the photon structure function by Field, Kapusta, and Poggioli using ideas quite similar to those above. See J.H. Field, F. Kapusta, and L. Poggioli, Phys. Lett. B **181**, 362 (1986); Z. Phys. C **36**, 121 (1987). J.R. Forshaw, Phys. Lett. B **285**, 354 (1992), uses the approach of Field *et al.* to derive a formula for $\sigma_{\rm inel}^{\gamma p}$ similar to that in Eq. (22), but with the unphysical restriction that $\sigma_{q\bar{q}}$ in the last term include only purely perturbative contributions with no soft component. This approximation overlooks the necessary continuity of the expression under variations of Q_0^2.

[21] See, for example, J.G. Morfin and W.-K. Tung, Z. Phys. C **52**, 13 (1991).

[22] L. Durand and R. Lipes, Phys. Rev. Lett. **20**, 637 (1968); T.T. Chou and C.N. Yang, *ibid.* **20**, 1213 (1968); Phys. Rev. **170**, 1591 (1968).

[23] *Handbook of Mathematical Functions*, edited by M. Abramowitz and I. Stegun (Dover, New York, 1965), Secs. 9.6, 11.4.44.

[24] The proper variable for the Regge expansion is $s - m_\rho^2$ and not s. The former is proportional to $\cos\theta_t$, the cosine of the t-channel scattering angle. It is also proportional to $E_{\gamma,\mathrm{lab}}$, the variable used in the expansions reported in [15].

[25] P. l'Heureux, B. Margolis, and P. Valin, Phys. Rev. D **32**, 1681 (1985); M. Block, R. Fletcher, F. Halzen, B. Margolis, and P. Valin, *ibid.* **41**, 978 (1990); in *Elastic and Diffractive Scatterings* [10], pp. 31 and 238.

[26] The $1/p_{\perp,0}^2$ scaling of σ_{soft} introduced above for geometrical reasons is related by duality arguments to the $1/M_V^2$ scaling of the Vp total cross sections for excited vector states introduced in the vector-dominance model to obtain Bjorken scaling of the $\gamma\gamma$ cross sections. The quantities $1/p_{\perp 0}^2$ and $1/M_V^2$ are related on the average through Eq. (13). Similarly, the proportionality of $d\mathcal{P}_{q\bar{q}}$ to $1/p_{\perp 0}^2$ corresponds to the $1/M_V^2$ variation of the γV couplings assumed in vector dominance. See, for example, J.J. Sakurai and D. Schildknecht, Phys. Lett. **40B**, 121 (1972); **41B**, 489 (1972); A. Bramón, E. Etim, and M. Greco, *ibid.* **41B**, 609 (1972).

[27] A different derivation of this decomposition based on the Abramovski-Kancheli-Gribov cutting rules of Reggeon field theory or perturbative QCD is given by R. Blankenbecler, A. Capella, J. Tran Thanh Van, C. Pajares, and A.V. Ramallo, Phys. Lett. **107B**, 106 (1981).

[28] T.K. Gaisser and T. Stanev, Phys. Lett. B **219**, 375 (1989).

[29] A. Donnachie and G. Shaw, in *Electromagnetic Interactions of Hadrons*, edited by A. Donnachie and G. Shaw (Plenum, New York, 1978), Vol. 2, Chap. 3.

[30] M. Glück, K. Grassie, and E. Reya, Phys. Rev. D **30**, 1447 (1985).

[31] M. Drees and K. Grassie, Z. Phys. C **28**, 451 (1985).

[32] M. Glück, E. Reya, and A. Vögt, Phys. Rev. D **46**, 1973 (1992); Z. Phys. C **53**, 127 (1992).

[33] J.F. Owens, Phys. Rev. D **30**, 943 (1984).

[34] See, e.g., R.J. DeWitt, L.M. Jones, J.D. Sullivan, D.E. Willen, and H.W. Wyld, Jr., Phys. Rev. D **19**, 2056 (1979); **20**, 1751(E) (1979).

[35] The data used in the fits were from H. Meyer *et al.*, Phys. Lett. **33B**, 189 (1970), 1.66 GeV $\leq \sqrt{s} \leq$ 3.59 GeV; D.O. Caldwell *et al.*, Phys. Rev. Lett. **25**, 609 (1970), 2.9 GeV $\leq \sqrt{s} \leq$ 5.89 GeV; and D.O. Caldwell *et al.*, *ibid.* **40**, 1222 (1978), 5.89 GeV $\leq \sqrt{s} \leq$ 19.3 GeV. The data below $\sqrt{s} = 3$ GeV in Figs. 1 and 3 are from Meyer *et al.* and from T.A. Armstrong *et al.*, Phys. Rev. D **5**, 1640 (1972), 1.18 GeV $\leq \sqrt{s} \leq$ 2.96 GeV.

[36] E. Eichten, I. Hinchliffe, K. Lane, and C. Quigg, Rev. Mod. Phys. **56**, 579 (1984).

[37] For the parton distributions we will use, the parton densities at small x are not large enough for the saturation or recombination effects discussed by L.V. Gribov, E.M. Levin, and M.G. Ryskin, Phys. Rep. **100**, 1 (1983), to be important, and we will ignore them. See, however, the discussion in [9]. The saturation effects ultimately limit the growth of the parton distributions for $x \to 0$.

[38] D. Duke and J. Owens, Phys. Rev. D **26**, 1600 (1982).

[39] With the scaling forms we have used for the soft $q\bar{q} - p$ cross section and overlap function, and the $q\bar{q}$ parton distributions, the final cross section depends on Q_0 only through the restriction that $p_\perp$ be larger in the integral for $\sigma_{\mathrm{QCD}}^{q\bar{q}}$ than the larger of $p_{\perp 0}$ and $p_{\perp,\mathrm{min}}$. The effects are minimal for $p_{\perp,\mathrm{min}}^2 \gg Q_0^2$, e.g., less than 0.3% in the cross sections at $\sqrt{s}$=200 GeV for 280 MeV< Q_0 <400 MeV, a range which gives average masses for the $q\bar{q}$ system in the gap between the $\rho(770)$ and the $\rho(1450)$. If we were to take Q_0 >400 MeV, we would have to include excited vector states explicitly, and rescale.

[40] We pick this energy for the comparison because it is clearly in the flat region near the minimum in $\sigma^{\gamma p}$, but at an energy at which $s\bar{s}$ contributions to the rising component of the cross section, which we treat at full strength, are not yet large. The suppression is greater at lower energies.

[41] There is some tradeoff possible in such models between the energy dependence of cross sections induced by the growth of parton distributions at small x and that put in explicitly in the growing Regge term (compare, for example, Block *et al.* [25] and N.N. Nikolaev, in *Elastic and Diffractive Scatterings* [10], p. 95). It is therefore not generally possible to fix the parameters uniquely without independent information on at least one of these contributions.

[42] R.J. Glauber, in *Lectures in Theoretical Physics*, edited by W. Britten and L.G. Dunham (Interscience, New York, 1959), Vol. 1, p. 315; R.J. Glauber and G. Matthiae, Nucl. Phys. **B21**, 135 (1970).

[43] See H. Pi, Ph.D. dissertation, University of Wisconsin, 1989, Sec. 7, for a detailed discussion of the parallel case of p-air scattering.

[44] We note that the discrepancy would be removed if the ρ structure functions f_i^ρ were about 15% smaller than the pion functions f_i^π at low $p_\perp$, with the downward scaling corresponding to the observed ~15% reduction of the observed ρp cross section relative to the $\pi^\pm p$ cross sections [15].

[45] J.R. Forshaw and J.K. Storrow, Phys. Rev. D **46**, 4955 (1992).

[46] H. Abramowicz, K. Charchula, and A. Levy, Phys. Lett. B **269**, 458 (1991).